Chemistry and Physics of Lipids 211 (2018) 4–15

Contents lists available at ScienceDirect

Chemistry and Physics of Lipids

journal homepage: www.elsevier.com/locate/chemphyslip

The effect of mutations in the lid region of *Thermomyces lanuginosus* lipase on interactions with triglyceride surfaces: A multi-scale simulation study

Nathalie Willems[a], Mickäel Lelimousin[a,b], Jakob Skjold-Jørgensen[c], Allan Svendsen[c,*], Mark S.P. Sansom[a,*]

[a] Department of Biochemistry, University of Oxford, South Parks Road, Oxford OX1 3QU, United Kingdom
[b] CERMAV UPR5301, CNRS and Université Grenoble Alpes, BP 53, 38041 Grenoble cedex 9, France
[c] Novozymes A/S, Krogshoejvej 36, 2880 Bagsvaerd, Denmark

ARTICLE INFO

Keywords:
Molecular dynamics
Lipase
Conformational dynamics
Surface interactions
Mutagenesis
Triglyceride surfaces

ABSTRACT

Lipases naturally function at the interface formed between amphiphilic molecules and the aqueous environment. *Thermomyces lanuginosus* lipase (TLL) is a well-characterised lipase, known to exhibit interfacial activation during which a lid region covering the active site becomes displaced upon interaction with an interface. In this study, we investigate the effect the amino acid sequence of the lid region on interfacial binding and lid dynamics of TLL. Three TLL variants were investigated, a wild-type variant, a variant containing an esterase lid region (Esterase), and a Hybrid variant, containing both wild-type lid residues and esterase lid residues. Multiple coarse-grained molecular dynamics simulations revealed that the interfacial binding orientation of TLL was significantly affected by the nature of amino acids in the lid region, and atomistic simulations indicated effects on the structural dynamics of the lid itself. The atomistic simulations, as well as steered molecular dynamics simulations, also indicated that the Esterase lid region was less flexible than the wild-type lid region, whereas the Hybrid variant displayed superior lid flexibility and stability in the open conformation both at the interface, and in aqueous solution. Additional experiments performed to investigate the activity and binding behaviour of the lipase variants indicated a slightly higher specific activity for the Hybrid variant compared to the wild-type variant, correlating the observations of increased lid flexibility. Together, these results are in line with previous experimental studies, highlighting the importance of the nature of the amino acid residues within the functional lid region of lipases, particularly regarding interfacial binding orientation, activation, and structural stability.

1. Introduction

Lipases are enzymes that catalyse the hydrolysis of ester bonds in triglycerides at a water-lipid interface (Schmid and Verger, 1998). A structural motif commonly referred to as the “lid” region plays an important role in the activation of the lipase upon interaction with the lipid interface (Brzozowski et al., 1991a; Reis et al., 2009b; Sarda and Desnuelle, 1958). The interfacial interaction is thought to result in a conformational change in the lipase causing the lid region to become displaced, exposing hydrophobic residues within the lid region, and revealing the underlying catalytic site (Fig. 1A) (Derewenda et al., 1994, 1992; Grochulski et al., 1994). This conformational change is referred to as interfacial activation and allows substrate to access the binding pocket of the enzyme.

Mutating the amino acids present in the lid regions of lipases has been shown to affect lipase activity, enantioselectivity, and thermostability, generating variants with advantageous properties, such as enhanced catalytic efficiency (Bezzine et al., 1999; Secundo et al., 2006; Yu et al., 2014). *Thermomyces lanuginosus* lipase (TLL) is a well-characterised lipase with biotechnological applications in the detergent, cosmetics, and pharmaceutical industries (Houde et al., 2004). The lid region spans residues 82–98, and the catalytic triad consists of S146, H258, and D201 (Fig. 1A) (Brzozowski et al., 2000; Derewenda et al., 1994).

Recently, it was shown that mutating the residues within the lid region of TLL affected the catalytic properties of the lipase in different environments (Skjold-Jørgensen et al., 2014). Five different lipase variants were constructed based on a helix region (residues 71–77) present in a structurally similar esterase ferulic acid esterase (FAEA) (Fig. 1C) (Skjold-Jørgensen et al., 2014). Complete replacement of the lid region of TLL by the FAEA helix resulted in a decrease in interfacial activity and an increase in activity against water-soluble substrate, exhibiting esterase properties (Esterase variant). Conversely, selected mutations within the lid region of TLL resulted in both an increase in

* Corresponding authors.
E-mail addresses: asv@novozymes.com (A. Svendsen), mark.sansom@bioch.ox.ac.uk (M.S.P. Sansom).

http://dx.doi.org/10.1016/j.chemphyslip.2017.08.004
Received 19 April 2017; Received in revised form 25 July 2017; Accepted 8 August 2017
Available online 15 August 2017
0009-3084/

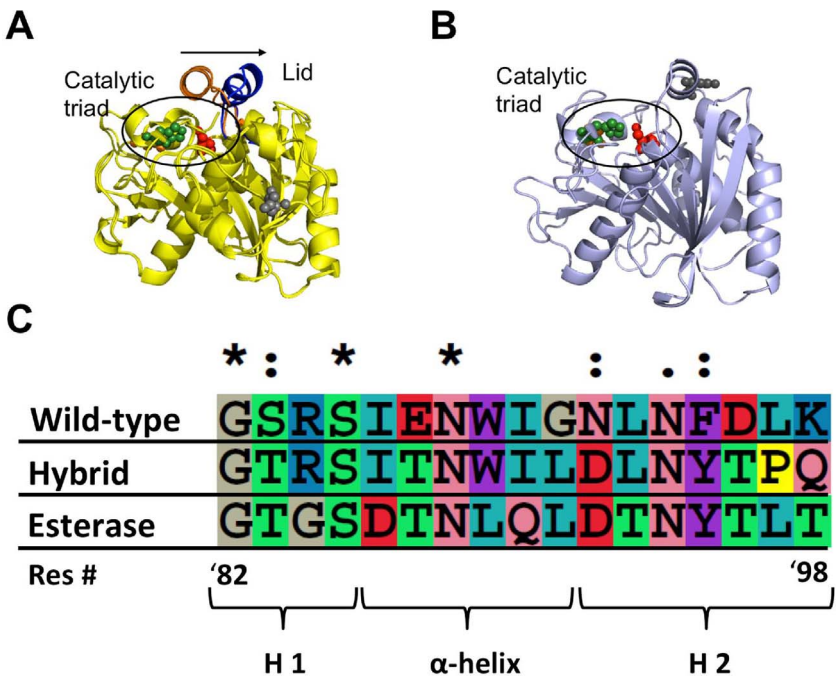

Fig. 1. (A) Structural alignment of the crystal structures of the open (blue lid; PDB: 1DTE) and closed (orange lid; PDB: 1DT5) conformations of TLL shown as cartoon representations (Brzozowski et al., 2000). The catalytic triad (S146, H258, and D201) is shown as red, green, and orange van der Waals spheres, respectively. The N33 glycosylation site is shown as grey van der Waals spheres, and the arrow indicates the motion of the lid region upon interfacial activation of TLL. **(B)** The crystal structure of ferulic acid esterase (FAEA) (McAuley et al., 2004). The catalytic triad (S133, D194, H247) is shown in the same respective colours and representations as in **(A)**. The N79 glycosylation site is shown as grey van der Waals spheres. **(C)** Multiple sequence alignment of the three selected variants generated by Jorgensen et al. (Skjold-Jørgensen et al., 2014). Asterisks denote a single fully conserved residue; colons denote regions of conserved residues that are highly similar, and the period denotes a region of conserved residues with a low degree of similarity. The nature of the mutations within the lid region are described in (Skjold-Jørgensen et al., 2014). Briefly, the wild-type variant retained the original amino acid sequence of the TLL lid region, while the Esterase lid variant contained all the amino acid residues in the FAEA helix region. The Hybrid variant contained mutations that are naturally present in the FAEA esterase helix region, as well as amino acids present in the wild-type TLL lid region. The "PQ" motif at positions 97 and 98 is commonly found in many hydrolase enzymes related to FAEA, and was therefore included in the lid sequence of the Hybrid variant. (For interpretation of the references to colour in this figure legend, the reader is referred to the web version of this article.)

interfacial activity, and activity against water-soluble substrate, compared to the wild-type enzyme (a variant referred to as "Hybrid"). The Hybrid therefore exhibited both lipase and esterase activity, reflecting the mixed amino acid composition of the mutated lid region. The wild-type variant naturally exhibited high activity at the interface, and very little activity against water-soluble substrate. Currently, it is not well understood why the Hybrid variant exhibited reproducibly higher lipase *and* esterase activity than wild-type TLL and wild-type FAEA (Skjold-Jørgensen et al., 2014).

In this context, molecular dynamics (MD) simulations provide a useful method to probe the underlying dynamic processes determining the activity of the TLL variants, and their behaviour in different environments. MD simulations have provided valuable insight into the structural mechanisms underlying interfacial activation of TLL at the interface, as well as solvent effects on interfacial activation of the lipase (Jensen et al., 2002; Peters et al., 1997; Rehm et al., 2010; Santini et al., 2009). Therefore, the analysis of selected TLL variants over different simulation timescales may provide information on how the mutated lid residues affect lipase binding behaviour and lid dynamics with respect to activation.

In this study, both coarse-grained (CG) and atomistic (AT) MD simulations were used to investigate the binding behaviour and structural dynamics of the wild-type, Esterase and Hybrid TLL variants. Two different environments were studied: an interfacial environment in which a triglyceride interface was present, and an aqueous environment. These environments were chosen in order to reproduce the experimental assays performed in (Skjold-Jørgensen et al., 2014), as well as experimental assays performed in this study, investigating the lipase activity and binding behaviour. Interestingly, the interfacial orientation of bound TLL at the triglyceride interface was heavily influenced by the nature of the amino acids present within the lid region. Accordingly, the experimental binding assays revealed differences in the association of wild-type and Hybrid variants with a lipid interface, showing sensitivity to the residue composition of the lid region. The structural flexibility of the lid region was also affected by the mutations, resulting in much larger energetic barrier to lid displacement in the Esterase variant compared to the wild-type and Hybrid variants. Furthermore, this energetic barrier was found to be lower in the Hybrid variant compared to the wild-type variant, rationalising the experimentally observed increase in lipase activity exhibited by the Hybrid variant compared to the wild-type lipase (Skjold-Jørgensen et al., 2015, 2014). Together, the simulation results suggest that the nature of the residues within the lid region of TLL plays a critical role in both structural dynamics and interfacial interactions, resulting in considerably different activity profiles. This information is valuable for generating lipase variants with advantageous properties, such as increased stability and activity in aqueous environments, and can be used to inform further mutagenesis experiments.

2. Methods

All simulations were performed with GROMACS 4.6.5 simulation software (www.gromacs.org).

2.1. Coarse-grained simulations: proteins models

Crystal structures for the open (PDB: 1DTE) and closed (PDB: 1DT5) forms of wild-type TLL were downloaded from the PDB (Brzozowski et al., 2000). The mutagenesis tool in PyMOL was used to generate structures for the TLL variants (The PyMOL Molecular Graphics System, Version 1.4 Schrödinger, LLC.). The side chain rotamer with the highest occupancy and least number of clashes with the surrounding protein environment was chosen for each mutation. The Martinize.py script was used to convert the TLL variants structures to CG representation (available at: http://md.chem.rug.nl/index.php/tools2/proteins-and-bilayers). All CG simulations were performed using the Martini 2.2 forcefield and the Martini polarisable water model (Jong and Singh, 2012; Marrink et al., 2004; Monticelli et al., 2008; Yesylevskyy et al., 2010). The Martini forcefield maps, on average, four non-hydrogen atoms to a single particle, and was employed using standard parameters for bonding and non-bonding interactions. The ElNeDyn (EDM) elastic network model was used to maintain secondary and tertiary structure of the proteins (Jong and Singh, 2012; Marrink et al., 2007; Periole et al., 2009). Parameterisation of the EDM networks was based on 50 ns atomistic (AT) simulations of each protein in water. Atomistic models of the lipase variants were generated using the *pdb2gmx* tool in GROMACS (simulation parameters below).

2.2. Coarse-grained simulations: system setup

A supported triglyceride system was constructed to mimic the systems employed in the experimental study (using microtitre plate assays) (Skjold-Jørgensen et al., 2014). The triglyceride interface was generated by performing self-assembly simulations of 501 trioleate triglyceride molecules randomly inserted in a simulation box (final dimensions: $10 \times 10 \times 15\ nm^3$). The parameters for the CG trioleate model were kindly supplied by Vattulainen et al. (Vuorela et al., 2010). The self-assembled layer was then placed directly above a hydrophobic support and the system was solvated (Gobbo et al., 2013). The system was energy minimised for 1000 steps using the steepest descent algorithm, followed by equilibration for 10 ps in the NPT ensemble at 298 K and 1 bar (Berendsen et al., 1984). Production simulations of 500 ns were subsequently performed, indicating that the layer was stable on the surface. A leapfrog algorithm was used to integrate Newton's equations of motion, with a time step of 20 fs. The Berendsen thermostat was used for temperature coupling with a weak coupling constant of 1.0 ps (Berendsen et al., 1984). Anisotropic pressure coupling was applied using the Berendsen barostat with a coupling constant of 3.0 ps, and a compressibility of $0.5 \times 10^{-5}\ bar^{-1}$ in x and y, and $3.0 \times 10^{-5}\ bar^{-1}$ in the z-direction (Gobbo et al., 2013).

The CG lipase structures were then individually placed 3 nm above the supported triglyceride layer and counter ions were added to neutralise the charge of the systems. Three different starting orientations were simulated to minimise any bias occurring from the initial orientation of the enzyme (Fig. 2). Since the lid region is thought to be central in mediating interfacial interactions, the lipase molecules were rotated 90° about the Y-axis for each orientation, such that the lid region was in a different position relative to the interface. The systems were subsequently energy minimised, and equilibrated for 10 ps in the NPT ensemble. Five replicate simulations of 2 μs each were performed for each lipase variant, including the open and closed form of the wild-type TL lipase, resulting in a fifteen replicate ensemble for each of the lipase molecules.

2.3. Atomistic simulations

All AT simulations were performed using the GROMOS 54A7 forcefield and SPC water model (Berendsen et al., 1981; Oostenbrink et al., 2005, 2004). A triglyceride layer was formed by randomly inserting 731 tributyrin molecules into a $10 \times 10 \times 5\ nm^3$ simulation box. The tributyrin GROMOS 54A7 AT forcefield topology and coordinate files were downloaded from the Automated Topology Builder website (http://compbio.biosci.uq.edu.au/atb/) (Canzar et al., 2013; Koziara et al., 2014; Malde et al., 2011). After steepest descent energy minimisation, 1 ns of NVT equilibration at 298 K was performed, after which the z-dimension of the box was extended to 10 nm and the system solvated with SPC water. An additional 1 ns of NPT simulation ensured that the density of tributyrin layer equilibrated to 1026 g/L (the experimental value at 298 K is 1027 g/L (Eiteman and Goodrum, 1994)). The AT lipase structures were then individually placed 1 nm above the pre-formed tributyrin layer, and water molecules were added. The systems were then energy minimised and equilibrated for 100 ps in the NPT ensemble. Production simulations consisting of three repeat simulations for each variant were performed for 100 ns each, totalling nine simulations. Three repeat simulations of 100 ns were also performed for the lipase variants in water, allowing comparison of the interfacial behaviour.

2.4. Steered MD simulations

Steered MD (SMD) simulations were performed using the Plumed 2.1 plugin for GROMACS (Bonomi et al., 2009; Tribello et al., 2014). The equilibrated, initially closed, structures of each lipase variant in water were used as a starting point, applying the same AT simulation parameters as above. A distance collective variable (CV) was chosen to investigate the opening motion of the lid region of the TL lipase variants. This CV was defined as the distance between the centre of mass (COM) of the Cα atoms of I255, positioned distal to the lid region, and of residue 87, present in lid region (further details below). A harmonic bias potential was applied to the CV, moving at a constant velocity of $0.06\ nm\ ns^{-1}$ with a spring stiffness of $1000\ kJ\ mol^{-1}$. The limit values for the distance CV were measured from the closed and open crystal

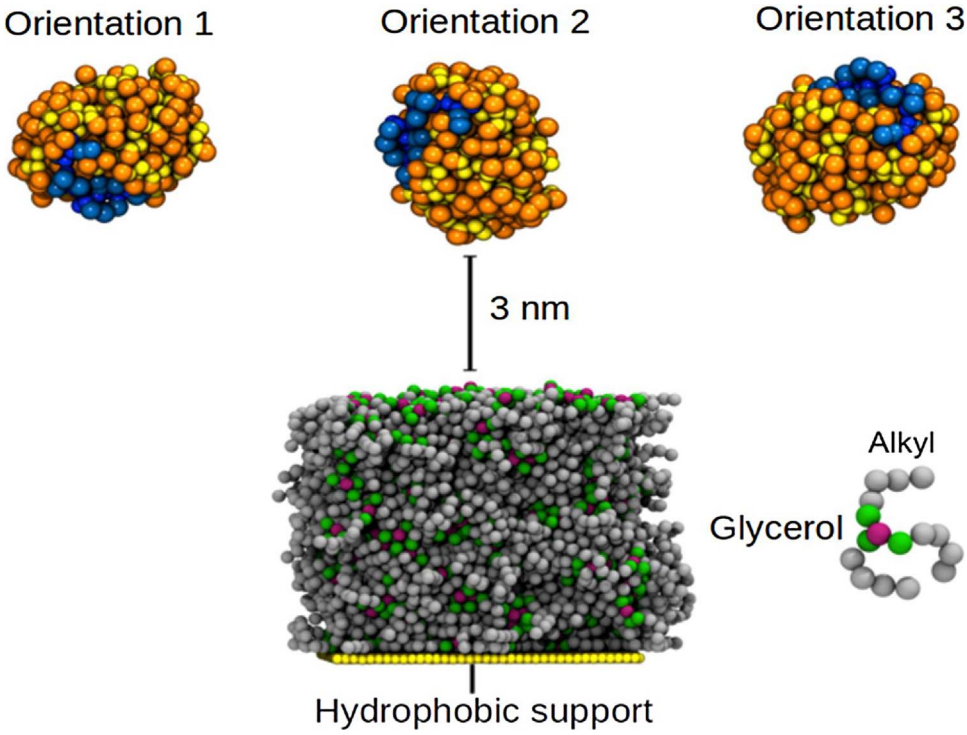

Fig. 2. Setup of the TLL-triglyceride CG simulations. Three different starting orientations of TLL positioned above the supported triglyceride layer were simulated (2 μs). The lipase is shown as yellow and orange van der Waals representations; the lid region is shown in blue. The triglyceride molecules are shown as green (esters), grey (alkyl), and purple (glycerol) van der Waals spheres. The support surface is shown as yellow van der Waals spheres. (For interpretation of the references to colour in this figure legend, the reader is referred to the web version of this article.)

structures of wild-type TLL (Brzozowski et al., 2000).

Additional SMD simulations were also performed for the Esterase variant after association with the tributyrin layer. These were initiated from the final frame of an unbiased AT simulation of the Esterase variant with the tributyrin interface (100 ns), applying identical SMD simulation parameters as above. The SMD simulations were performed by either applying position restraints to the protein atoms (Fc = 1000 kJ mol^{-1}) except those within the lid region (residues 82–98), or no position restraints at all.

2.5. Lipase activity assays

The lipase activity assays were conducted similar to the method described in (Skjold-Jørgensen et al., 2014). Briefly, 96-well non-binding microtiter plates (Corning, catalogue no. 3995) were coated with 100 nmol of triolein (CAS Registry No. 8001-25-0) and 100 nmol of pNP-decanoate (CAS Registry No. 1956-09-8). Ten µl of the enzyme solution was transferred to 190 µL of buffer (100 mM Tris pH 8 + 2 mM $CaCl_2$) on a separate 96-well non-binding microtiter plate, minimising unspecific adsorption of lipase to the well surface. Plates were subsequently incubated for 10 min at room temperature. 150 µL of the enzyme dilution was then transferred to the coated lipase assay plate with a multipipette (Liquidator RAININ, Mettler Toledo). The coated assay plate was immediately placed in the plate reader (SpectraMax Plus 384, Molecular Devices), and the increase in absorbance due to the *p*-nitrophenolate anion was measured at 405 nm. The assay was conducted at 25 °C for 15 min, measuring absorbance every 12 s. Assays were performed in triplicate. The specific activity was calculated from the steepest slope.

2.6. Binding assays

Differences in binding between the lipase variants to lipid layers of olive oil were investigated in a set-up similar to the lipase assay described above. Enzyme samples were diluted to 50 µg/mL in 25 mM MOPS pH 7.5. 190 µL buffer (100 mM Tris pH 8 + 2 mM $CaCl_2$) was added to 10 µL enzyme sample in a non-binding microtiter plate (Corning). 150 µL of the sample volume was added to a different microtiter plate coated with 100 nmol olive oil. Binding of lipase to the olive oil surface was then determined by measuring the residual activity of unbound lipase in the supernatant over time (between 2 and 40 min) relative to the initial activity at time zero. This was done by assaying 20 µL of supernatant in 100 µL reaction buffer (50 mM Tris pH 7.5 + 0.4% Triton X–100 + 10 mM $CaCl_2$) and calculating activity from the initial rate of pNP-butyrate hydrolysis at 405 nm.

3. Results

3.1. Interfacial interactions of TL lipase variants with triglycerides explored via CG simulations

The effect of lid mutations on the catalytic properties of the TL lipase has been characterised experimentally (Skjold-Jørgensen et al., 2016, 2015, 2014). In this study, CG simulations and experimental activity and binding assays were used to investigate the dynamic properties of selected TLL mutants in more detail. Corresponding to previous experimental data, the Hybrid variant exhibited a higher rate of lipase activity and higher specific activity than the wild-type variant at the lipid interface, while the Esterase variant displayed very little activity at the interface (Fig. 3A and B). These measurements are consistent with hydrolytic activity of the lipase variants on water-soluble substrate in bulk solution, in which the Hybrid variant displayed the largest activity at both low and high concentrations (above critical micelle concentration) of water soluble pNP-butyrate, whereas the Esterase variant displayed the lowest activity at all concentrations. Interestingly, the wild-type variant exhibited a higher degree of association with the lipid interface than the Hybrid variant, specifically from ~20 min onwards (Fig. 3C), suggesting that the wild-type variant associated more strongly with the interface over time. Additionally, the wild-type variant displayed a slightly higher activity than the Hybrid variant against water-soluble substrate in the presence of non-ionic surfactant (Fig. S1).

In the CG simulations, all the lipase variants associated with the triglyceride layer, and did not dissociate from the interface once bound. However, the number of repeat simulations in which the lipase associated with the interface differed for each of the variants (Table S1). Interestingly, the Esterase variant displayed the smallest number of binding events within the 15 replicate ensemble, in which one binding event represents association of the lipase with the interface in one simulation. The Hybrid variant displayed the most binding events, associating with the triglyceride surface in 14/15 simulations (Table S1). This observation correlates with the experimental binding data (Fig. 3C) suggesting that the Hybrid and wild-type variants initially bind the interface in a similar way, exhibiting similar interfacial orientations (Fig. 4A), although the Hybrid variant exhibited a higher number of binding events within the overall CG ensemble (Table S1). This contrasts the experimental observation that the wild-type variant binds the interface more strongly than the Hybrid variant over time, which may be related to sampling limitations in the CG simulations, restricted by the short simulation time (2 µs) and the relatively small number of replicate simulations performed within each ensemble.

The experimental data also show that the Hybrid variant displayed a slightly higher specific activity compared to the wild-type variant (Fig. 3B), correlating with previous observations that the lid region may affect the overall interfacial enzyme activity exhibited (Skjold-Jørgensen et al., 2016, 2014). The Esterase variant, on the other hand, displayed very little activity and binding to the interface within these experiments (data were omitted from Fig. 3) (Skjold-Jørgensen et al., 2014). This is in line with the CG simulations, in which the Esterase variant displayed the least number of binding events out of the three variants.

Representative images for the bound lipase molecules taken from the CG simulations are shown in Fig. 4. These indicate that the orientation of the lid region at the interface differed for the bound lipase variants. The lid regions of the wild-type closed variant and the Esterase variant were much more solvent exposed, typically pointing away from the interface, whilst the lid regions of the Hybrid and wild-type open variant were embedded within the interface, buried from the surrounding solvent (Fig. 4A). The interfacial interactions exhibited by the lipase variants were characterised in more detail by calculating the average number of contacts between the lipase and the triglyceride molecules (Fig. 4B). Only those simulations in which the lipase associated with the interface were considered for each ensemble of simulations. These interaction data were normalised by averaging the total number of contacts across the repeat simulations within each ensemble.

Both polar and hydrophobic amino acids mediated contacts with the interface for all of the variants, representing interactions with both polar glycerol groups and non-polar carbon tails of the triglyceride molecules. Importantly, the interfacial contacts consistently mapped to residues within the lid region and surrounding amino acid residues for each of the lipase variants, as can be seen by comparing the reference orientations with the contact maps shown in Fig. 4B and C. Interestingly, the lid region of the Hybrid lipase, of both esterase and lipase character, displayed the largest number of interactions with the interface compared to other amino acid residues within this variant, suggesting that the lid mainly remained in contact with the interface once bound. This observation correlates with the large interfacial activity displayed by the Hybrid variant within the experimental assays (Fig. 3A), given that interactions between the lid and interface are necessary to bring about interfacial activation and lipase activity (Brzozowski et al., 1991b, 2000; Sarda and Desnuelle, 1958; Skjold-Jørgensen et al., 2015, 2014). The most commonly interacting residues

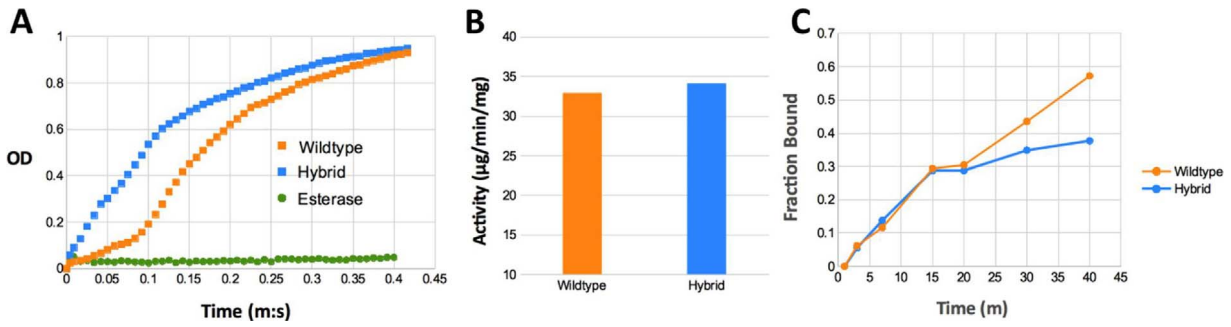

Fig. 3. (A) Time evolution of the optical density (OD) increase at pH 8, displaying the interfacial lipase activity of the wild-type, Hybrid, and Esterase variants on pNP-decanoate (100 nmol) embedded in a triolein layer (100 nmol). **(B)** Specific activities of wild-type and Hybrid variants calculated from the steepest slopes of the data shown in (A). **(C)** Time course of the binding behaviour of the wild-type and Hybrid variants on olive oil in microtiter plates, measured in 100 mM Tris at pH 8. Error bars denote standard deviation (assays were performed in triplicate). Given the small level of activity of measured for the Esterase variant, this enzyme was omitted from the (B) and (C).

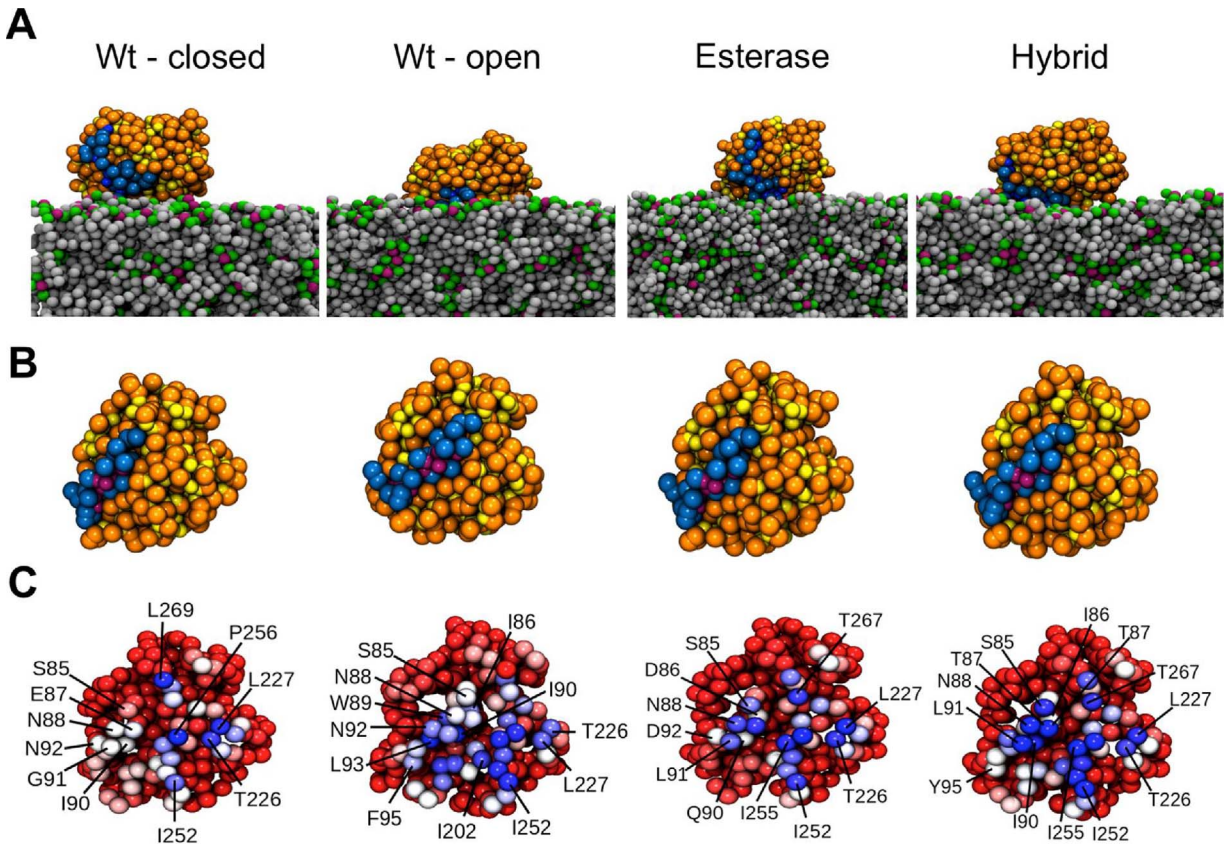

Fig. 4. (A) Representative binding orientations of lipase variants when bound to a triglyceride interface observed from CG simulations. The lid of TLL is coloured in blue, and rest of the protein in orange (amino acid side chains) and yellow (amino acid backbone). The triglyceride carbon tails are coloured in grey, ester groups in green, and glycerol in purple. **(B)** Reference orientations of the lipase variants for the contact residue maps shown in **(C)**. Contacts between the lipase molecules and the triglyceride molecules were calculated within a 0.8 nm cut-off for each repeat simulation, and normalised across the ensemble for each of variants. The contacts are displayed on van der Waals representations of the lipase variants using a blue/white/red colour scale, where red = no contact and blue = greatest number of contacts. Both closed and open models of the wild-type variant were simulated; the Esterase and Hybrid variants were simulated in their closed state (lid covering active site). (For interpretation of the references to colour in this figure legend, the reader is referred to the web version of this article.)

of the Hybrid lipase included the mutated lid residues, such as G91L and E87T, but also include wild-type residues such as I86 and N88. Conversely, the mutated residues within the lid region of the Esterase variant, such as I86D, I90Q, and N92Q, mediated relatively fewer contacts with the interface than other residues within the lid region, suggesting that the negatively charged substitutions could diminish interfacial contact via the lid region of Esterase.

The different interfacial orientations of the lipase variants on the triglyceride surface were further analysed by evaluating the rotational and translation motions exhibited by the variants during association with the interface. The rotational motions of the lipase were described by a defined angle between the lipase and the interface (*Rzz*). This was obtained by calculation of a rotation matrix with respect to a reference orientation of the lipase at the interface (Fig. 5A). The translational motions were described by measuring the centre of mass (COM) distance (*d*) between the lipase and triglyceride interface over simulation time.

Consistent with previous observations, the association process and interfacial orientations differed between the lipase variants. The collective data allowed calculation of a 2-dimensional density landscape representing the normalised density of the binding orientations exhibited by the variants, as a function of *d* and *Rzz* (Fig. 5B).

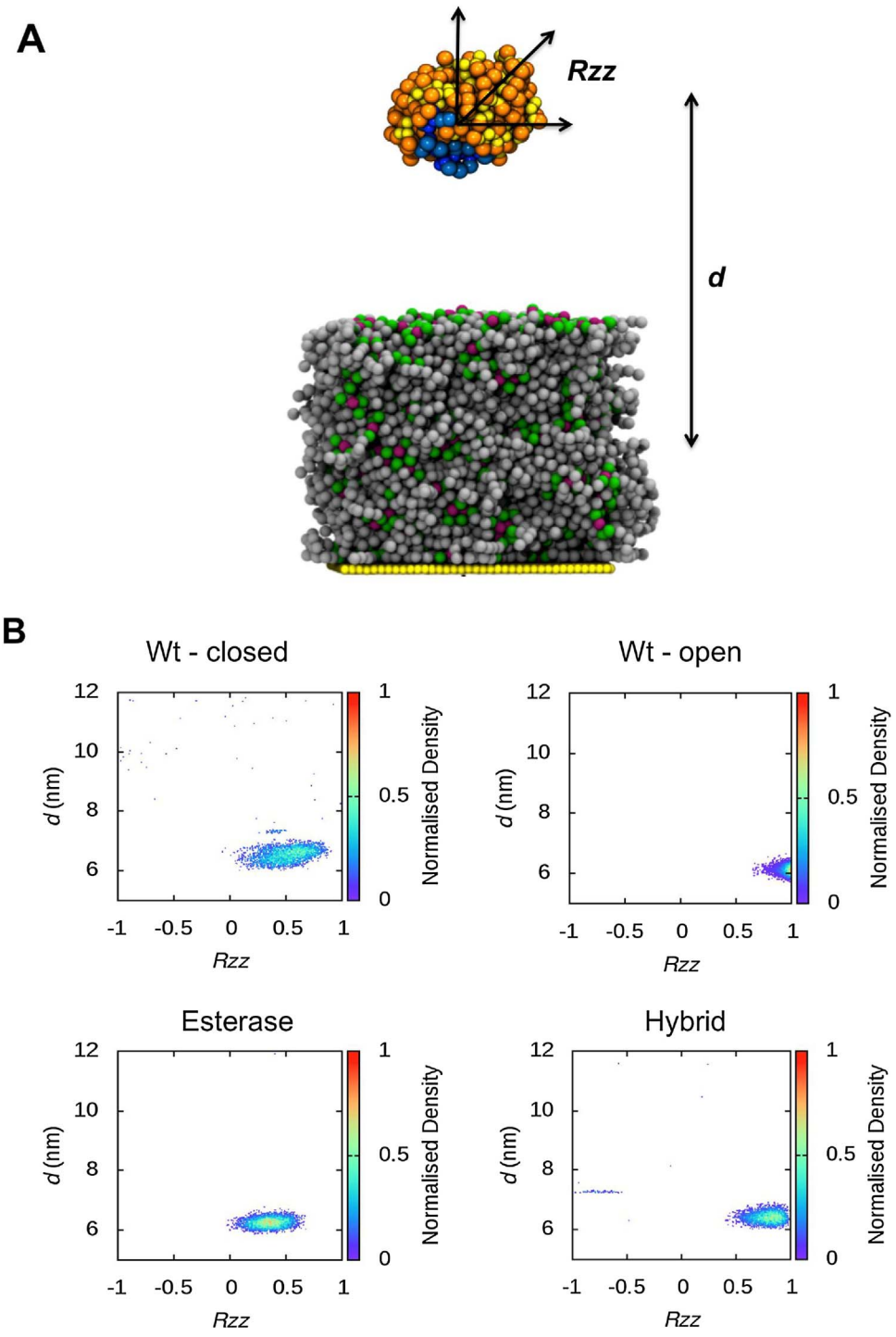

Fig. 5. (A) Initial system configuration for the CG simulations of TLL binding to a triglyceride layer. The figure schematically represents the CVs (*d* and *Rzz*) used to describe the rotational and translational motion exhibited by the lipase during the simulation. The metric *d* was calculated as the z-component of the distance between the COM of the protein relative to the COM of the layer. A rotation matrix was calculated as a function of the *Rzz* angle that defines the transition from a given orientation of the enzyme (orange arrows) to a reference orientation. When $Rzz = 1$, the enzyme adopts the orientation of the reference structure. The same colour scheme as in Fig. 4A is used. **(B)** 2D density landscapes calculated for CG simulation of lipase variants with a triglyceride layer as a function of *d* and *Rzz*. Representative data are shown in Fig. S1. The top of the triglyceride layer corresponds to the bottom of the map ($\sim d = 5$). (For interpretation of the references to colour in this figure legend, the reader is referred to the web version of this article.)

Accordingly, the density landscapes indicate a substantial difference in the average interfacial enzyme orientation adopted by the variants, particularly the Esterase variant compared to the wild-type open and Hybrid variants. This can be seen from variation in the average *Rzz* value for the Esterase mutant, as well as closed wild-type lipase, producing a distribution between $Rzz = 0$–0.5, compared to $Rzz = 0.5$–1 for the wild-type open and Hybrid variants (Fig. 5B).

The overall wider distributions of binding orientations for Esterase and the closed wild-type variants suggest that both the nature of the residues within the lid region, as well as their orientation (exposed in the open wild-type variant), are important determinants of overall interfacial orientation. These data suggest that an altered binding orientation could be a factor in the diminished interfacial activity of the Esterase variant observed experimentally, relative to the wild-type and Hybrid variants (Skjold-Jørgensen et al., 2016, 2015). Furthermore, the frequently sampled buried orientation of Hybrid lid region within the interface also suggests that lipase activation is favoured in this variant as a function of its lid residue composition. Together, these results correspond well with the experimental activity data presented in Fig. 3A and B (Skjold-Jørgensen et al., 2014), in which the wild-type and Hybrid variants exhibited the highest interfacial lipase activity, whilst the Esterase variant exhibited very little.

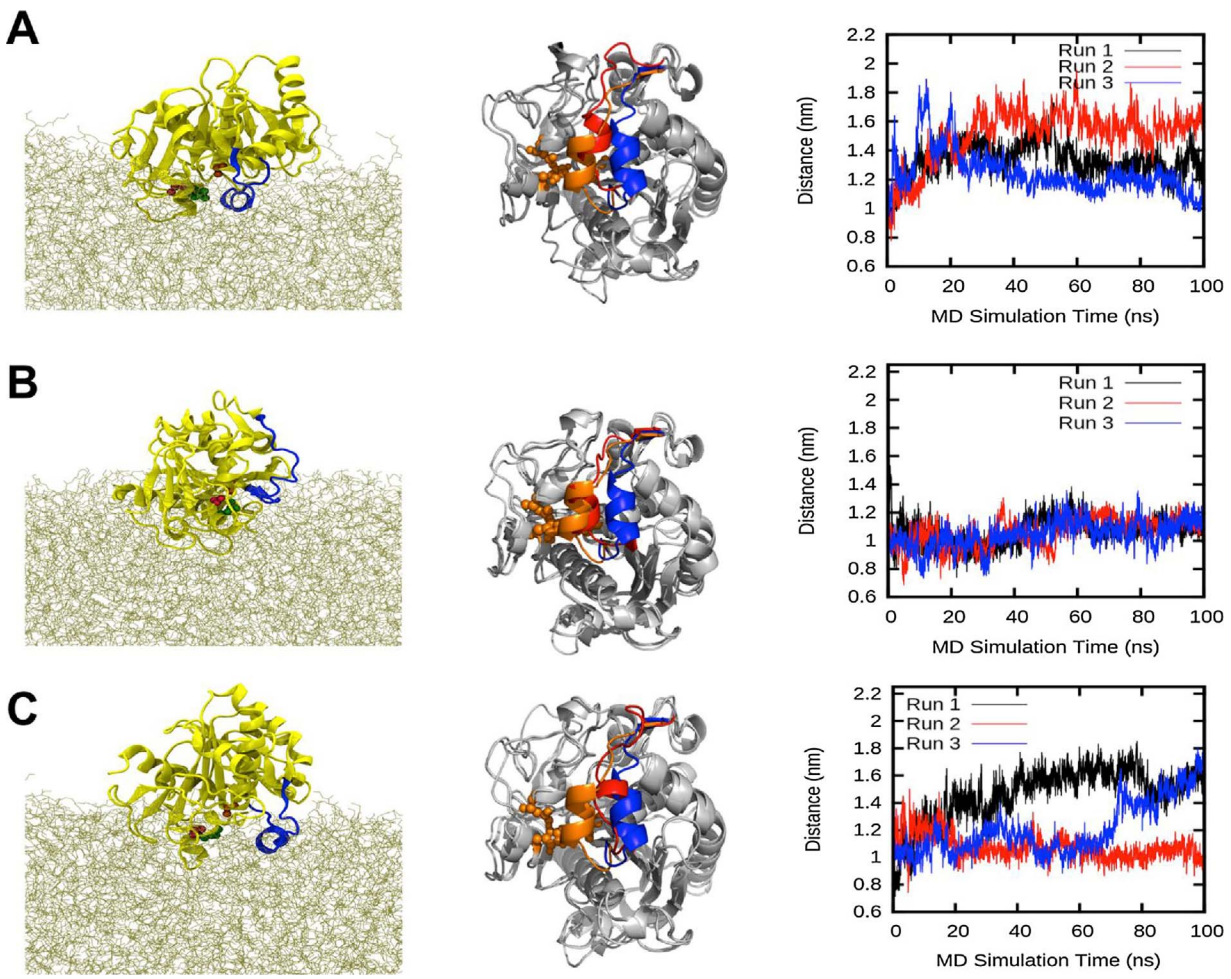

Fig. 6. *Left*: Bound orientations of initially closed wild-type **(A)**, Esterase **(B)** and Hybrid lipase **(C)** variants shown for the final frame of AT simulations with a tributyrin interface. The protein is shown as a yellow cartoon; the lid is coloured blue. The catalytic residues, S146, H258, D201, are shown as van der Waals spheres coloured in red, green, and orange respectively. *Middle*: Top down view of the representative simulated lipase structures (100 ns; lid coloured red) aligned with the closed (lid coloured orange) and open (lid coloured blue) crystal structures of wild-type TLL. The structures represent Run 2 of the 3 repeat simulations for the wild-type variant, and Run 1 for the Esterase and Hybrid variants. *Right*: Time evolution of the distance between the Cα atoms of residue 87 (within lid region) and residue 255 (neighbouring region) measuring the closed-open lid transition, shown for the 3 repeat simulations. (For interpretation of the references to colour in this figure legend, the reader is referred to the web version of this article.)

3.2. Conformational dynamics of interfacially bound TLL variants

Atomistic (AT) simulations of the lipase interactions with triglycerides surfaces were performed in order to study the structural motions of the lipase variants in more detail. The AT simulations (3 repeats) showed a general agreement with the CG simulations regarding lipase orientation at the interface (Fig. 6).

Interestingly, both the initially closed forms of the wild-type and Hybrid variants displayed partial interfacial activation during the simulations, whereas the lid region of Esterase remained firmly closed for all repeat simulations. This can be seen from alignment of the final lipase structures with the closed and open crystal structures of wild-type TLL, and is reflected in calculation of the COM distance travelled by the lid region during the simulations (Fig. 6). The similar structural motions exhibited by the wild-type and Hybrid variants suggests that the lid mutations within the Hybrid did not impact lid mobility or flexibility to a great extent.

However, the Hybrid variant exhibited some variation in conformational motions within the 3 repeat simulations; specifically, one repeat simulation (Run 2) did not result in lid displacement within the 100 ns simulation time (Fig. 6C). Interestingly, the Hybrid lid sequence contains a proline residue at the 97th position that could impact local lid flexibility, although it is possible that extension of the simulation could result in lid displacement over a longer time scale. The Esterase lipase did not exhibit any interfacial activation upon association with the triglyceride interface, correlating with the very low interfacial activity observed experimentally (Skjold-Jørgensen et al., 2014).

A further three repeat AT simulations were performed of the lipase variants in an initially open conformation, investigating lid flexibility as a possible factor underlying altered activity. The final bound orientations of the lipase variants are shown in Fig. 7A.

Interestingly, the lid region of the Esterase variant did not return to the closed position in any of the simulations, correlating with previous observations of reduced lid flexibility, although some structural deviation could be observed, particularly for the third repeat simulation (Figs. 7B and Fig. S3A). Conversely, the lid region of the wild-type lipase exhibited significant closure in each repeat simulation, most likely due to initial solvent exposure of the hydrophobic residues within this region prior to lipase binding, which is thought to drive lid closure (Fig. 7A) (Rehm et al., 2010). The Hybrid variant did not exhibit this closing motion in any of the simulations, where the initially open lid conformation was apparently stable even prior to lipase association with the interface (Fig. 7C). This stability is also reflected in a constant value of the distance metric used to measuring the lid transition, indicating that the Hybrid lid region maintained its open position at ~2.1 nm for the duration of the simulations (distance measured as I255-R87Cα COM distance) (Fig. 7C). The altered structural dynamics of the Hybrid lid region compared to the wild-type variant are thus a

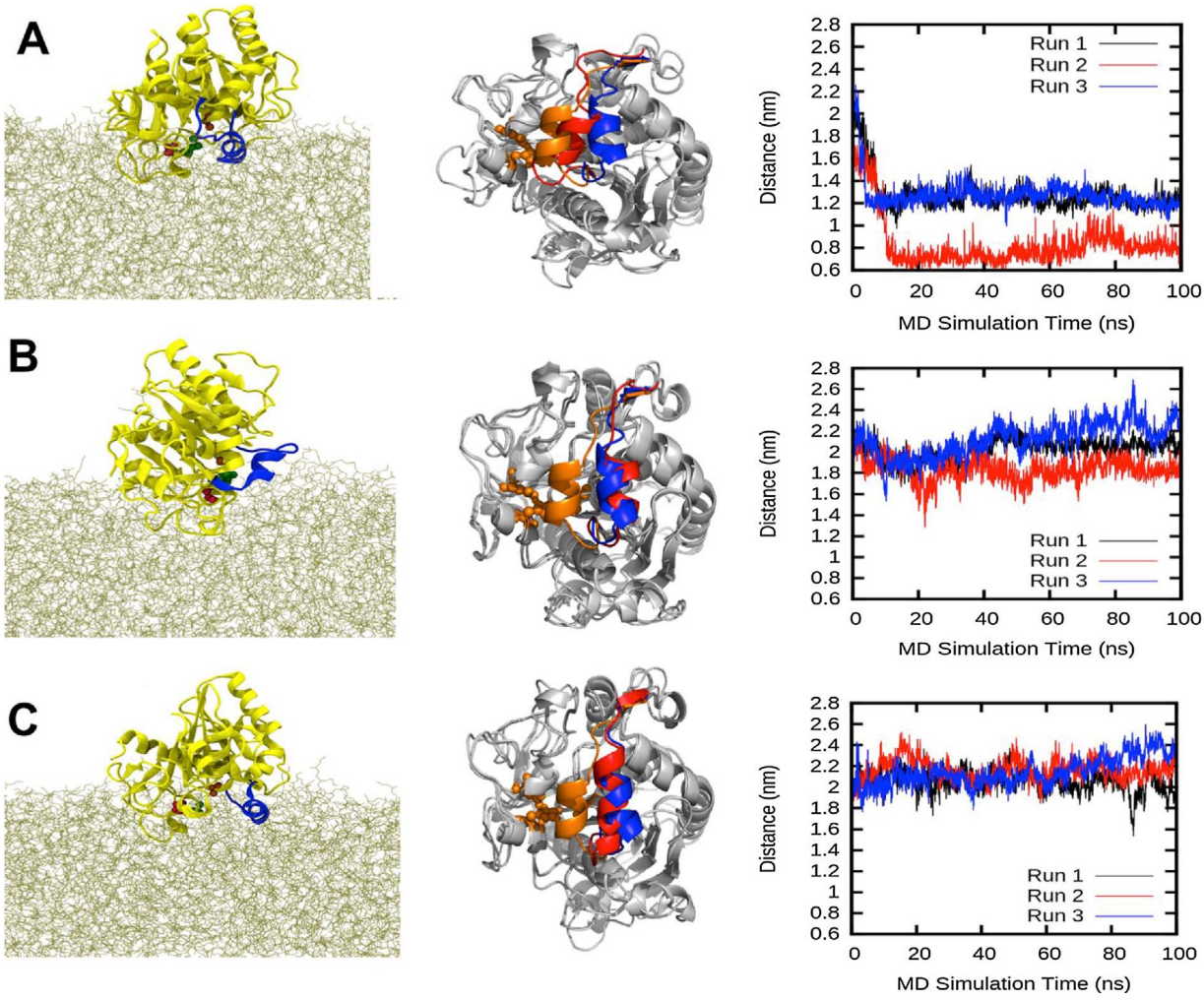

Fig. 7. *Left*: Bound orientations of initially open wild-type **(A)**, Esterase **(B)** and Hybrid lipase **(C)** variants extracted from the final frame of AT simulations with a tributyrin interface. The same colour scheme as in Fig. 5 is used. *Middle*: Top down view of the representative simulated lipase structures (100 ns; lid coloured red) aligned with the closed (lid coloured orange) and open (lid coloured blue) crystal structures of wild-type TLL. The structures represent Run 1 of the 3 repeat simulations for all variants. *Right*: Time evolution of the distance between the Cα atoms of residue 87 (within lid region) and residue 255 (neighbouring region) measuring the closed-open lid transition, shown for the 3 repeat simulations. (For interpretation of the references to colour in this figure legend, the reader is referred to the web version of this article.)

likely determinant of the observed enhanced activity of Hybrid against water-soluble substrate (Skjold-Jørgensen et al., 2014).

3.3. Conformational dynamics of lipase variants in water

In order to compare the structural motions observed for the lipase variants at the tributyrin interface, additional AT simulations were performed in water. The simulations showed good agreement with earlier observations of the different structural dynamics observed for the lid regions of the lipase variants (Figs. S5 and S6). Specifically, simulation of the initially closed form of the Esterase variant did not result in significant lid displacement in any of the repeat simulations, although slightly increased lid flexibility was observed in the aqueous environment (Fig. S5B). Similarly, the wild-type lipase also maintained a closed conformation in this high dielectric constant environment, consistent with observations that the lipase is inactive in the absence of an interface (Fig. S5A) (Skjold-Jørgensen et al., 2014). In contrast, the lid region of Hybrid was more mobile, even exhibiting partial activation during one of the repeat simulations (Fig. S5C). However, more variation in lid displacement was observed when starting from an initially open conformation, particularly for the wild-type and Esterase variants (Figs. S7 and S8). Here, the Esterase variant remained fully open for 2/3 repeat simulations, whilst the wild-type lipase exhibited either partial or full closure of the lid region in all repeat simulations (Fig. S8A and B). Conversely, the lid region of the Hybrid variant remained relatively open for 2/3 repeat simulations, coinciding with previous observations of superior stability of the open conformation of this lipase in solution (Fig. S7C).

The observed differences in lid dynamics of the variants highlight the importance of residue composition on the overall structural stability and dynamics of the lid region. The distinct distribution of hydrophobic residues within the α-helix of the Hybrid lid domain is similar to that of wild-type TLL, suggesting that the hinge regions of the lid play a key role in lid mobility. Experimentally, the differences in activity between the variants have been attributed to the underlying energetic barrier to lid opening, which appears to be sufficiently low in Hybrid to allow catalysis on water-soluble substrate (Fig. 3A and B) (Skjold-Jørgensen et al., 2014). This was explored further using steered MD simulations to provide initial estimates of the energetic barrier associated with the lid opening process for each of the variants.

To capture the opening motion of the lid, a distance CV was defined between the Cα atom of residue 87 in the lid region (E87 in wild-type) and the Cα atom of a distally located residue (I255) (Fig. 8A). These residues were previously identified as a good metric for lid activation in fluorescence studies of TLL in different solvents (Skjold-Jørgensen et al., 2015). SMD simulations were performed for each of the lipase

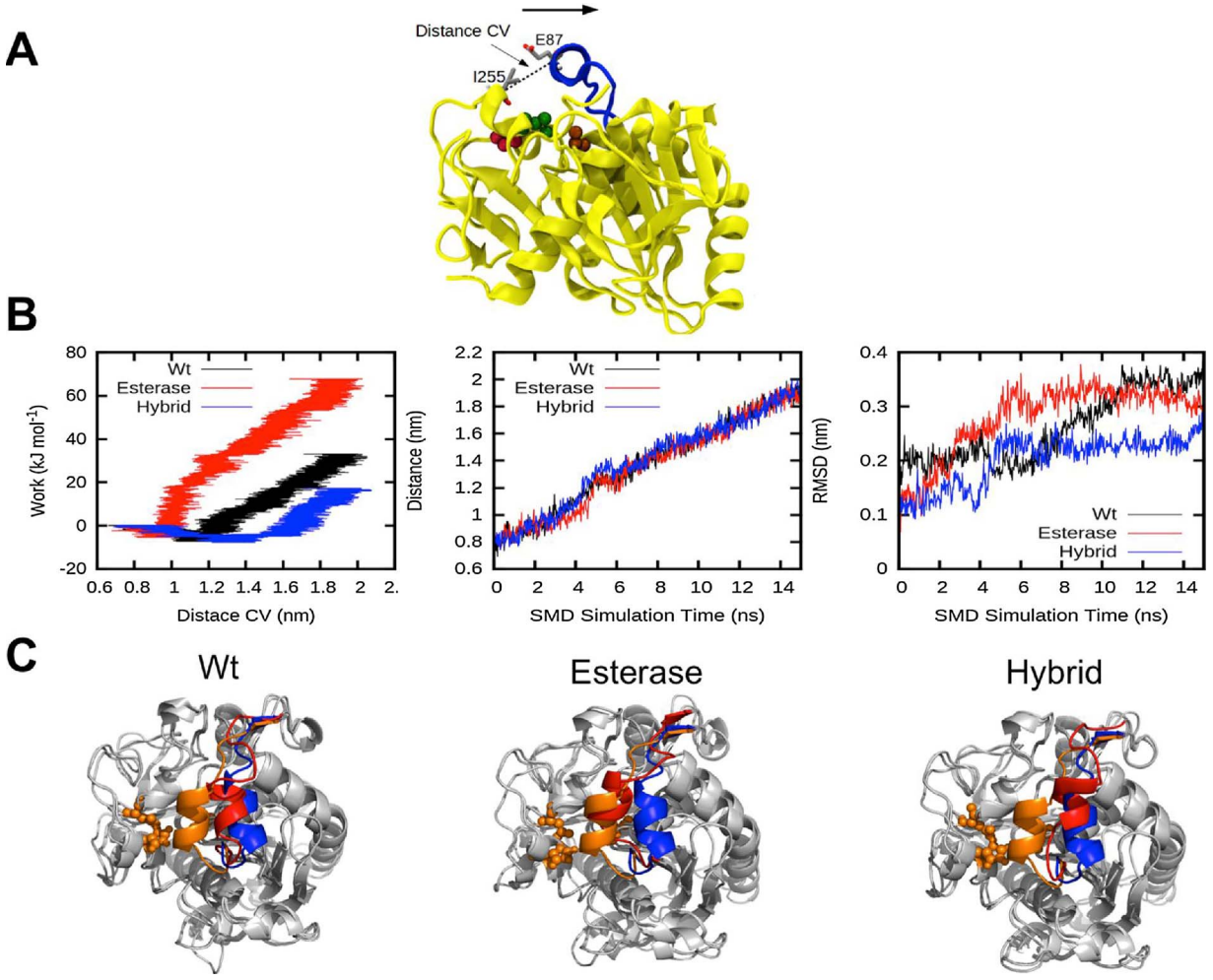

Fig. 8. (A) Definition of a distance CV for SMD simulations of lipase variants in water. The CV measures the COM distance between the Cα atoms of I255 and E87 (wild- type sequence). The same colour scheme as in Fig. 5 is used. **(B)** The work profiles (*left*), time evolution of the CV (*middle*), and time evolution of the RMSD of the Cα atoms within the lid region (*right*) of the lipase variants calculated for the SMD simulations of the lid opening process in water. **(C)** Images of the final frame of the SMD simulations showing each of the lipase variants at 15 ns (lid coloured red). The lipase structures were aligned with the closed (lid coloured orange) and open (lid coloured blue) crystal structures of the wild-type lipase, showing a top-down view of the structures. (For interpretation of the references to colour in this figure legend, the reader is referred to the web version of this article.)

variants in water. The resulting work profiles indicated that the largest amount of work was performed for simulation of the Esterase variant, whilst the lowest work was performed for the Hybrid variant (Fig. 8B). This is in line with previous observations of reduced lid flexibility in the Esterase lipase, where structural analysis shows the Esterase lid region was barely displaced during the SMD simulation (Fig. 8C).

Evolution of the distance CV for the Esterase lipase is thought to be due to the biasing force displacing a neighbouring loop region that is close to the 87th residue within the lid, rather than displacement of the lid region itself (Fig. S10). This suggests that the intermolecular forces mediating lid position are stronger than the biasing force used during the SMD simulation (1000 kJ mol^{-1}). In contrast, the lid region of the Hybrid variant was most easily displaced in comparison with the wild-type and Esterase variants, coinciding with previous observation of increased lid mobility for Hybrid (Fig. 8B).

Analysis of the contacts between the lid region and the neighbouring protein residues indicate that hydrophobic interactions between residues such as I90-I255 and L93-I202 were broken as the lid is pushed away during the SMD simulations, exposing these hydrophobic residues to the solvent (Fig. S9). Furthermore, visualisation of residue position and orientation within the lid region at the end of the SMD simulations indicate that the residues become more solvent exposed (Fig. S10). The resultant work profiles match previous observations from unbiased AT-MD simulations, suggesting constraints on lid dynamics for the Esterase variant, compared to increased lid mobility for the Hybrid variant.

3.4. Steered MD simulations of lipase variants at a triglyceride interface

In addition to simulating the lid opening process of the lipase variants in water, it is important to characterise the motions of the lid region when the lipase is in contact with the triglyceride interface. Additional SMD simulations were performed to investigate these motions for the Esterase variant. These were initiated from the final structure of the bound lipase molecule from unbiased AT simulations with the natural substrate interface (Fig. 6). The same SMD protocol was performed as detailed in the previous section. SMD simulations of the bound forms of the wild-type and Hybrid variants were not performed given that these variants displayed degrees of interfacial activation during unbiased simulations with the triglyceride interface, and thus would be difficult to compare to the SMD simulations performed in water, in which the starting structures were fully closed.

SMD simulations of the Esterase variant at the interface resulted in an increase in the amount of work performed to sample lid displacement compared to SMD simulations in water. However, the lid region was still not significantly displaced at the interface. To overcome this issue, position restraints were applied to all atoms within the lipase except those within the lid region. This protocol enabled greater

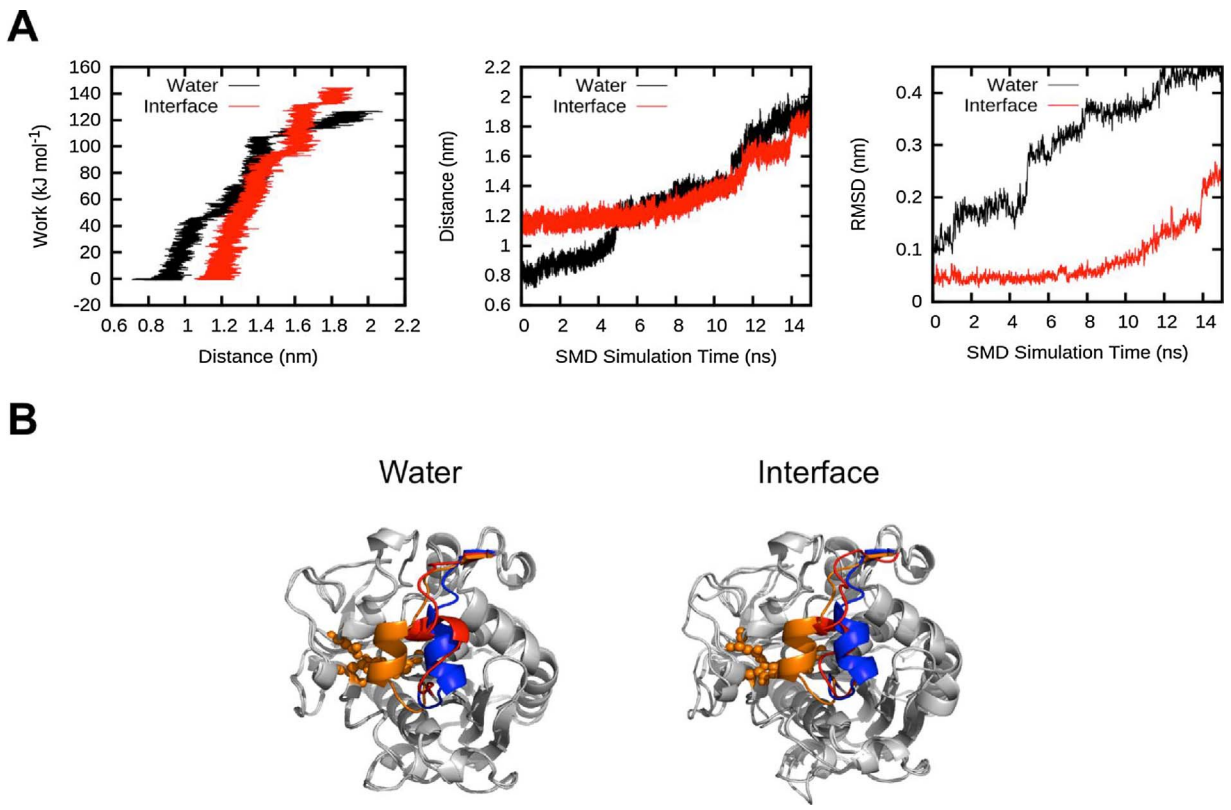

Fig. 9. SMD simulations were performed for the Esterase lipase variants in water and at a tributyrin interface with position restraints as defined in the main text. **(A)** The calculated work profiles (*left*), time evolution of the lid distance CV (*middle*), and time evolution of the RMSD of the Cα atoms within the lid region (*right*). **(B)** Protein structures of the lipase variant obtained from the final frame of SMD simulations in both water and at the interface (lid coloured red), aligned with the closed (lid coloured orange) and open (lid coloured blue) crystal structures of the wild-type lipase. (For interpretation of the references to colour in this figure legend, the reader is referred to the web version of this article.)

extension of the distance CV and subsequent displacement of lid region in the Esterase variant in water and at the interface (Fig. 9).

The work evolved during the SMD simulations indicate that the lid was most easily displaced in water compared to the interface. This feature could underlie the enhanced activity of Esterase towards water-soluble substrate compared to substrate embedded in an interface (Skjold-Jørgensen et al., 2014).

4. Discussion

Existing experimental data suggest that amino acid substitutions within the lid region of the TL lipase influence interfacial activation and catalytic activity (Skjold-Jorgensen et al., 2016; Skjold-Jørgensen et al., 2016, 2015, 2014). Other studies of different lipases have demonstrated similar effects, highlighting the critical role of the lid region in enzyme activity and substrate specificity (Secundo et al., 2006; Wang et al., 2015; Yu et al., 2014). Here, CG and AT simulations were used to investigate how mutation of the lid region of TLL affects interfacial interactions with a natural substrate, as well as conformational dynamics at the interface and in solution.

Both the CG and AT simulations of the lipase mutants with the triglyceride interface suggested a distribution of interfacial binding orientations. Specifically, the Esterase variant, which exhibited esterase activity, consistently displayed an orientation in which the lid region pointed away from the triglyceride interface, interacting with the surrounding solvent (Skjold-Jørgensen et al., 2014). In contrast, the Hybrid variant, of lipase and esterase character, displayed an average orientation in which the lid region was buried within the interface, consistent with the open form of the wild-type lipase (Figs. 4 and 5). This buried interfacial orientation is in line with experimental studies of wild-type TLL at phospholipid interfaces, as well as other hydrophobic surfaces (Hedin et al., 2002; Sonesson et al., 2008). Contact analysis of the CG simulations indicated that the mutations in the Esterase variant, including I86D, I90Q, and N92Q, formed fewer contacts with the interface than other residues within the lid region. These charged and negative substitutions could affect the orientation of the lipase variant at the interface and diminish interfacial contact via the lid region of Esterase. The altered interfacial orientation of the Esterase, as highlighted by Fig. 5B, could therefore attributed to the lid mutations, and could be related to the negative substitutions within the lid region. However, further simulations and analysis are necessary to confirm whether the altered lid sequence is responsible the difference in the observed interfacial orientation. Furthermore, the difference in the triglyceride molecule used in the CG (trioleate) and AT (tributyrin) simulations limits comparisons between these interfaces, as the nature of the interface could affect the orientation adopted by the bound lipase molecule (Berg et al., 1998; Cajal et al., 2000a,b). It would be interesting to compare the binding mechanisms of the lipase variants with a long-chain triglyceride interface composed of trioleate at an atomistic level, both for validation of the CG simulation results, and for comparison with the short-chain triglyceride tributyrin interface.

The amino acid sequences within the mutated regions also appeared to affect the structural dynamics of the lid regions, particularly for the Esterase variant. AT simulations of both an initially closed and open form of the variants revealed that lid displacement and flexibility was significantly diminished in the Esterase variant. Similarly, experimental studies of other lipases with mutated lid regions were seen to influence the structural dynamics and thermostability of the mutated enzymes, implying that amino acid substitutions can affect lid region dynamics (Secundo et al., 2006; Yu et al., 2014). In contrast, the lid region of the Hybrid variant appeared to be more mobile relative to the wild-type and Esterase enzymes, and exhibited an open conformation in both interfacial and aqueous environments. These trends correlated with steered MD simulations investigating the lid opening motion of the

variants in water. Accordingly, the largest amount of work was evolved in simulations of the Esterase variant, whereas the smallest work was performed in simulations of the Hybrid variant. More generally, the considerable degree of lid rigidity displayed by the Esterase variant could be a distinguishing factor between a lipase and an esterase enzyme. Whilst most lipases exhibit lid flexibility, which is necessary to allow lid displacement (interfacial activation) and allow substrate access of long-chain triglycerides (Reis et al., 2009b; Sarda and Desnuelle, 1958), esterases generally do not require displacement of helical regions, where short-chain ester substrates are able to access the active site without conformational rearrangement (Aliwan et al., 1999; McAuley et al., 2004; Yu et al., 2014). This may be why the SMD simulations were unable to sample the lid opening process for the Esterase variant, suggesting that the lid mutations affect both the overall activity of the lipase, as well as its structural dynamics such as overall lid flexibility.

Accordingly, the enhanced flexibility of the lid region of the Hybrid variant, and its observed greater stability in the open conformation, compared to the wild-type variant most likely underlies its unique activity profile (Fig. 3A and B) (Skjold-Jørgensen et al., 2014). This has been related to a reduced energetic barrier for lid displacement in the Hybrid lipase compared to the wild-type, and is thought to be due to the specific residues within the hinge-regions of the lid (Skjold-Jørgensen et al., 2014). Additionally, the difference in lid dynamics displayed by the Hybrid and wild-type variants may also be related the substitution of the wild-type E87 residue with a threonine residue in the Hybrid variant. Previous computational studies of wild-type TLL suggested that displacement of the lid region to an open position in a high dielectric medium is unfavourable due to electrostatic repulsion between the E87 residue and negatively charged residues on the opposite side of the protein (Peters et al., 1997). Mutation of the E87 residue to a histidine residue in the study was observed to decrease the overall energy required to displace the lid, and even more so for a mutation to a positively charged lysine residue, resulting in an overall increase in energy gain upon activation (Peters et al., 1997). The electrostatic interactions between residues within the lid region and the surrounding protein environment are thus important in governing the lid opening process. The E87T mutation within the lid region of Hybrid could therefore result in reduced electrostatic repulsion experienced by the lid region upon lid activation relative to the wild-type variant. This may explain the superior stability exhibited by the Hybrid variant compared to the wild-type in unbiased AT simulations, particularly in simulations of initially open structures in water. Interestingly, investigation of the binding behaviour of the lipase variants indicated that the wild-type variant was more likely to remain bound to the interface compared to the Hybrid variant, whilst the Esterase variant displayed very little binding with the interface (Fig. 3C). Given that the Hybrid variant exhibited a higher interfacial activity and specific activity than the wild-type variant, one might initially expect that the Hybrid variant would bind the interface more strongly than the wild-type, given that interfacial interactions are important in activation and enzymatic activity of the lipase (Fig. 3) (Reis et al., 2009b). Related studies have indicated that the nature of the interface, specifically its lipid composition, has tremendous effects on both the association and activation of the bound lipase molecule (Cajal et al., 2000a,b; Hedin et al., 2002; Reis et al., 2009a, 2008). A study by Reis et al. (2008) employed tensiometry and interfacial shear rheology to show that the reaction products generated by the lipolytic action of lipases, such as *Sn*-2 monoglycerides, are very interfacially active, and can expel the lipase from the interface (Reis et al., 2008). Given that the Hybrid lipase exhibits a higher specific activity than the wild-type lipase, it is possible that the accumulation of *Sn*-2 monoglycerides at the interface occurs at a faster rate than with the wild-type lipase. Consequently, the higher concentration of *Sn*-2 monoglyceride may cause expulsion of the Hybrid from the interface resulting in an apparent smaller fraction of bound molecule compared to the wild-type (Fig. 3C). It is important to characterise the association behaviour and interfacial interactions of both the wild-type and Hybrid in more detail in order to clarify these experimental and computational data.

5. Conclusions

A combined simulation and experimental approach has provided insights into the conformational dynamics and interfacial interactions of TL lipase variants at triglyceride interfaces, and in solution. Factors such as altered interfacial binding orientations and lid dynamics may underlie the experimentally determined activity profiles for the wild-type, Esterase and Hybrid variants, and are closely related to the particular residue composition of the different lid regions (Skjold-Jørgensen et al., 2014). Additionally, lid glycosylation is known to play a part in lipase binding to the lipid interfaces (Peters et al., 2002; Pinholt et al., 2010). The lid region of the Esterase lipase contains a glycosylation site at the N89 residue of the N-high mannose type, as well as at the N33 residue of the same type (McAuley et al., 2004; Skjold-Jørgensen et al., 2014). The latter is also present within the wild-type and Hybrid variants (Skjold-Jørgensen et al., 2014). Simulations of the glycosylated variants will thus be important in providing a comprehensive description of lipase binding dynamics, and for comparison with the experiments.

Moreover, it would be of interest to characterise the energetics of the lid activation process for each of the variants in more detail. Although attempts were made to investigate this using SMD, this method suffers from limitations. First, the SMD simulations were unable to displace the lid region of the Esterase variant relative to the Hybrid and wild-type variants in water. When position restraints were applied, the SMD simulation was able to capture lid motion for the Esterase in water, resulting in a dramatic increase in the work performed. In contrast, similar work profiles were generated during both unrestrained and position restrained SMD simulations of the Esterase variant bound to the interface. These results indicate the both the distance CV and the nature of the SMD methods were insufficient to describe the lid activation process accurately. More rigorous enhanced sampling methods are required to firmly establish how lid mutations affect the energy landscape of lid displacement for the mutated proteins, both at the interface and in solution. These data could then be generalised for other lipases, providing a predictive tool that could be used in the rational design of lipase variants with attractive properties.

Conflict of interest

None.

Funding

This research was supported by the Biotechnology and Biological Sciences Research Council (BBSRC) [grant number BB/J014427/1].

Appendix A. Supplementary data

Supplementary data associated with this article can be found, in the online version, at http://dx.doi.org/10.1016/j.chemphyslip.2017.08.004.

References

Aliwan, F.O., Kroon, P.A., Faulds, C.B., Pickersgill, R., Williamson, G., 1999. Ferulic acid esterase-III from Aspergillus niger does not exhibit lipase activity. J. Sci. Food Agric. 79, 457–459. http://dx.doi.org/10.1002/(SICI)1097-0010(19990301)79:3<457:AID-JSFA283>3.0.CO;2-G.

Berendsen, H.J.C., Postma, J.P.M., van Gunsteren, W.F., Hermans, J., 1981. Interaction models for water in relation to protein hydration. In: Pullman, B. (Ed.), Intermolecular Forces, The Jerusalem Symposia on Quantum Chemistry and Biochemistry. Springer, Netherlands, pp. 331–342. http://dx.doi.org/10.1007/978-

94-015-7658-1_21.
Berendsen, H.J.C., Postma, J.P.M., van Gunsteren, W.F., DiNola, A., Haak, J.R., 1984. Molecular dynamics with coupling to an external bath. J. Chem. Phys. 81, 3684–3690. http://dx.doi.org/10.1063/1.448118.
Berg, O.G., Cajal, Y., Butterfoss, G.L., Grey, R.L., Alsina, M.A., Yu, B., Jain, M.K., 1998. Interfacial activation of triglyceride lipase from thermomyces (Humicola) lanuginosa: kinetic parameters and a basis for control of the lid. Biochemistry 37, 6615–6627.
Bezzine, S., Ferrato, F., Ivanova, M.G., Lopez, V., Verger, R., Carrière, F., 1999. Human pancreatic lipase: colipase dependence and interfacial binding of lid domain mutants. Biochemistry 38, 5499–5510. http://dx.doi.org/10.1021/bi982601x.
Bonomi, M., Branduardi, D., Bussi, G., Camilloni, C., Provasi, D., Raiteri, P., Donadio, D., Marinelli, F., Pietrucci, F., Broglia, R.A., Parrinello, M., 2009. PLUMED: A portable plugin for free-energy calculations with molecular dynamics. Comput. Phys. Commun. 180, 1961–1972. http://dx.doi.org/10.1016/j.cpc.2009.05.011.
Brzozowski, A.M., Derewenda, U., Derewenda, Z.S., Dodson, G.G., Lawson, D.M., Turkenburg, J.P., Bjorkling, F., Huge-Jensen, B., Patkar, S.A., Thim, L., 1991a. A model for interfacial activation in lipases from the structure of a fungal lipase-inhibitor complex.pdf. Nature 351, 491–494.
Brzozowski, A.M., Derewenda, U., Derewenda, Z.S., Dodson, G.G., Lawson, D.M., Turkenburg, J.P., Bjorkling, F., Huge-Jensen, B., Patkar, S.A., Thim, L., 1991b. A model for interfacial activation in lipases from the structure of a fungal lipase-inhibitor complex. Nature 351, 491–494. http://dx.doi.org/10.1038/351491a0.
Brzozowski, a M., Savage, H., Verma, C.S., Turkenburg, J.P., Lawson, D.M., Svendsen, a, Patkar, S., 2000. Structural origins of the interfacial activation in Thermomyces (Humicola) lanuginosa lipase. Biochemistry 39, 15071–15082.
Cajal, Y., Svendsen, A., Bolós, J., De Patkar, S., Alsina, M., 2000a. Effect of the lipid interface on the catalytic activity and spectroscopic properties of a fungal lipase. Biochimie 82, 1053–1061.
Cajal, Y., Svendsen, A., Girona, V., Patkar, S.a., Alsina, M.a., 2000b. Interfacial control of lid opening in Thermomyces lanuginosa lipase. Biochemistry 39, 413–423.
Canzar, S., El-Kebir, M., Pool, R., Elbassioni, K., Malde, A.K., Mark, A.E., Geerke, D.P., Stougie, L., Klau, G.W., 2013. Charge group partitioning in biomolecular simulation. J. Comput. Biol. 20, 188–198. http://dx.doi.org/10.1089/cmb.2012.0239.
Derewenda, U., Brzozowski, A.M., Lawson, D.M., Derewenda, Z.S., 1992. Catalysis at the interface: the anatomy of a conformational change in a triglyceride lipase. Biochemistry 31, 1532–1541. http://dx.doi.org/10.1021/bi00120a034.
Derewenda, U., Swenson, L., Wei, Y., Green, R., Kobos, P.M., Joerger, R., Haas, M.J., Derewenda, Z.S., 1994. Conformational lability of lipases observed in the absence of an oil-water interface: crystallographic studies of enzymes from the fungi Humicola lanuginosa and Rhizopus delemar. J. Lipid Res. 35, 524–534 (065/7).
Eiteman, M., Goodrum, J., 1994. Density and viscosity of low-molecular weight triglycerides and their mixtures. J. Am. Oil Chem. Soc. 71, 1261–1265. http://dx.doi.org/10.1007/BF02540548.
Gobbo, C., Beurroies, I., de Ridder, D., Eelkema, R., Marrink, S.J., De Feyter, S., van Esch, J.H., de Vries, A.H., 2013. MARTINI model for physisorption of organic molecules on graphite. J. Phys. Chem. C 117, 15623–15631. http://dx.doi.org/10.1021/jp402615p.
Grochulski, P., Li, Y., Schrag, J.D., Cygler, M., 1994. Two conformational states of Candida rugosa lipase. Protein Sci. 3, 82–91. http://dx.doi.org/10.1002/pro.5560030111.
Hedin, E.M.K., Høyrup, P., Patkar, S.a., Vind, J., Svendsen, A., Fransson, L., Hult, K., 2002. Interfacial orientation of Thermomyces lanuginosa lipase on phospholipid vesicles investigated by electron spin resonance relaxation spectroscopy. Biochemistry 41, 14185–14196.
Houde, A., Kademi, A., Leblanc, D., 2004. Lipases and their industrial applications. Appl. Biochem. Biotechnol. 118, 155–170.
Jensen, M.Ø., Jensen, T.R., Kjaer, K., Bjørnholm, T., Mouritsen, O.G., Peters, G.H., 2002. Orientation and conformation of a lipase at an interface studied by molecular dynamics simulations. Biophys. J. 83, 98–111. http://dx.doi.org/10.1016/S0006-3495(02)75152-7.
de Jong, D., Singh, G., 2012. Improved parameters for the martini coarse-grained protein force field. J. Chem. 9, 697.
Koziara, K.B., Stroet, M., Malde, A.K., Mark, A.E., 2014. Testing and validation of the Automated Topology Builder (ATB) version 2.0: prediction of hydration free enthalpies. J. Comput. Aided. Mol. Des. 28, 221–233. http://dx.doi.org/10.1007/s10822-014-9713-7.
Malde, A.K., Zuo, L., Breeze, M., Stroet, M., Poger, D., Nair, P.C., Oostenbrink, C., Mark, A.E., 2011. An automated force field topology builder (ATB) and repository: version 1.0. J. Chem. Theory Comput. 7, 4026–4037. http://dx.doi.org/10.1021/ct200196m.
Marrink, S.J., de Vries, A.H., Mark, A.E., 2004. Coarse grained model for semiquantitative lipid simulations. J. Phys. Chem. B 108, 750–760. http://dx.doi.org/10.1021/jp036508g.
Marrink, S.J., Risselada, H.J., Yefimov, S., Tieleman, D.P., De Vries, A.H., 2007. The MARTINI force field: coarse grained model for biomolecular simulations. J. Phys. Chem. B 111, 7812–7824.
McAuley, K.E., Svendsen, A., Patkar, S.A., Wilson, K.S., 2004. Structure of a feruloyl esterase from Aspergillus niger. Acta Crystallogr. Sect. D Biol. Crystallogr. 60, 878–887. http://dx.doi.org/10.1107/S0907444904004937.
Monticelli, L., Kandasamy, S.K., Periole, X., Larson, R.G., Tieleman, D.P., Marrink, S.-J., 2008. The MARTINI goarse-grained force field: extension to proteins. J. Chem. Theory Comput. 4, 819–834. http://dx.doi.org/10.1021/ct700324x.
Oostenbrink, C., Villa, A., Mark, A.E., van Gunsteren, W.F., 2004. A biomolecular force field based on the free enthalpy of hydration and solvation: the GROMOS force-field parameter sets 53A5 and 53A6. J. Comput. Chem. 25, 1656–1676.
Oostenbrink, C., Soares, T.a., van der Vegt, N.F.a., van Gunsteren, W.F., 2005. Validation of the 53A6 GROMOS force field. Eur. Biophys. J. 34, 273–284. http://dx.doi.org/10.1007/s00249-004-0448-6.
Periole, X., Cavalli, M., Marrink, S.-J., Ceruso, M.a., 2009. Combining an elastic network with a coarse-grained molecular force field: structure, dynamics, and intermolecular recognition. J. Chem. Theory Comput. 5, 2531–2543. http://dx.doi.org/10.1021/ct9002114.
Peters, G.H., Toxvaerd, S., Olsen, O.H., Svendsen, A., 1997. Computational studies of the activation of lipases and the effect of a hydrophobic environment. Protein Eng. 10, 137–147.
Peters, G.H., Svendsen, A., Langberg, H., Vind, J., Patkar, S., Kinnunen, P.K., 2002. Glycosylation of Thermomyces lanuginosa lipase enhances surface binding towards phospholipids, but does not significantly influence the catalytic activity. Colloids Surf. B Biointerfaces 26, 125–134. http://dx.doi.org/10.1016/S0927-7765(02)00030-9.
Pinholt, C., Fanø, M., Wiberg, C., Hostrup, S., Bukrinsky, J.T., Frokjaer, S., Norde, W., Jorgensen, L., 2010. Influence of glycosylation on the adsorption of Thermomyces lanuginosus lipase to hydrophobic and hydrophilic surfaces. Eur. J. Pharm. Sci. 40, 273–281. http://dx.doi.org/10.1016/j.ejps.2010.03.021.
Rehm, S., Trodler, P., Pleiss, J., 2010. Solvent-induced lid opening in lipases: a molecular dynamics study. Protein Sci. 19, 2122–2130. http://dx.doi.org/10.1002/pro.493.
Reis, P., Holmberg, K., Miller, R., Kragel, J., Grigoriev, D.O., Leser, M.E., Watzke, H.J., 2008. Competition between lipases and monoglycerides at interfaces. Langmuir 24, 7400–7407. http://dx.doi.org/10.1021/la800531y.
Reis, P., Holmberg, K., Miller, R., Leser, M.E., Raab, T., Watzke, H.J., 2009a. Lipase reaction at interfaces as self-limiting processes. Comptes Rendus Chim. 12, 163–170. http://dx.doi.org/10.1016/j.crci.2008.04.018.
Reis, P., Holmberg, K., Watzke, H., Leser, M.E., Miller, R., 2009b. Lipases at interfaces: a review. Adv. Colloid Interface Sci. 147–148, 237–250. http://dx.doi.org/10.1016/j.cis.2008.06.001.
Santini, S., Crowet, J.M., Thomas, a, Paquot, M., Vandenbol, M., Thonart, P., Wathelet, J.P., Blecker, C., Lognay, G., Brasseur, R., Lins, L., Charloteaux, B., 2009. Study of Thermomyces lanuginosa lipase in the presence of tributyrylglycerol and water. Biophys. J. 96, 4814–4825. http://dx.doi.org/10.1016/j.bpj.2009.03.040.
Sarda, L., Desnuelle, P., 1958. Actions of pancreatic lipase on esters in emulsions. Biochem. Biophys. Acta 30, 512–521.
Schmid, R.D., Verger, R., 1998. Lipases: interfacial enzymes with attractive applications. Angew. Chem. Int. Ed. 37, 1608–1633. http://dx.doi.org/10.1002/(SICI)1521-3757(19980619)110:12<1694:AID-ANGE1694>3.0.CO;2-3.
Secundo, F., Carrea, G., Tarabiono, C., Gatti-Lafranconi, P., Brocca, S., Lotti, M., Jaeger, K.-E., Puls, M., Eggert, T., 2006. The lid is a structural and functional determinant of lipase activity and selectivity. J. Mol. Catal. B Enzym. 39, 166–170. http://dx.doi.org/10.1016/j.molcatb.2006.01.018.
Skjold-Jørgensen, J., Vind, J., Svendsen, A., Bjerrum, M.J., 2014. Altering the activation mechanism in *Thermomyces lanuginosus* lipase. Biochemistry 53, 4152–4160.
Skjold-Jørgensen, J., Bhatia, V.K., Vind, J., Svendsen, A., Bjerrum, M.J., Farrens, D.L., 2015. Enzymatic activity of lipases correlates with polarity-induced conformational changes: a Trp-induced quenching (TrIQ) fluorescence study. Biochemistry. http://dx.doi.org/10.1021/acs.biochem.5b00328. 150618153605000.
Skjold-Jørgensen, J., Vind, J., Svendsen, A., Bjerrum, M.J., 2016. Lipases that activate at high solvent polarities. Biochemistry 55, 146–156. http://dx.doi.org/10.1021/acs.biochem.5b01114.
Skjold-Jorgensen, J., Vind, J., Svendsen, A., Bjerrum, M.J., 2016. Understanding the activation mechanism of Thermomyces lanuginosus lipase using rational design and tryptophan-induced fluorescence quenching. Eur. J. Lipid Sci. Technol. 118, 1644–1660. http://dx.doi.org/10.1002/ejlt.201600059.
Sonesson, A.W., Callisen, T.H., Brismar, H., Elofsson, U.M., 2008. Adsorption and activity of Thermomyces lanuginosus lipase on hydrophobic and hydrophilic surfaces measured with dual polarization interferometry (DPI) and confocal microscopy. Colloids Surf. B Biointerfaces 61, 208–215. http://dx.doi.org/10.1016/j.colsurfb.2007.08.005.
Tribello, G.A., Bonomi, M., Branduardi, D., Camilloni, C., Bussi, G., 2014. PLUMED 2: New feathers for an old bird. Comput. Phys. Commun. 185, 604–613. http://dx.doi.org/10.1016/j.cpc.2013.09.018.
Vuorela, T., Catte, A., Niemelä, P.S., Hall, A., Hyvönen, M.T., Marrink, S.-J., Karttunen, M., Vattulainen, I., 2010. Role of lipids in spheroidal high density lipoproteins. PLoS Comput. Biol. 6, e1000964. http://dx.doi.org/10.1371/journal.pcbi.1000964.
Wang, G., Liu, Z., Xu, L., Zhang, H., Yan, Y., 2015. Probing role of key residues in the divergent evolution of Yarrowia lipolytica lipase 2 and Aspergillus niger eruloyl esterase A. Microbiol. Res. 178, 27–34. http://dx.doi.org/10.1016/j.micres.2015.05.011.
Yesylevskyy, S.O., Schäfer, L.V., Sengupta, D., Marrink, S.J., 2010. Polarizable water model for the coarse-grained MARTINI force field. PLoS Comput. Biol. 6, e1000810. http://dx.doi.org/10.1371/journal.pcbi.1000810.
Yu, X.-W., Zhu, S.-S., Xiao, R., Xu, Y., 2014. Conversion of a Rhizopus chinensis lipase into an esterase by lid swapping. J. Lipid Res. 55, 1044–1051. http://dx.doi.org/10.1194/jlr.M043950.